# Effect of swift heavy ions irradiation in the migration of silver implanted into polycrystalline SiC

H.A.A. Abdelbagi[1,2*], V.A. Skuratov [3], S.V. Motloung4, E.G. Njoroge[1], M. Mlambo[1], J.B. Malherbe[1], J. H. O'Connell[5], T.T. Hlatshwayo[1]

[1]*Physics Department, University of Pretoria, Pretoria 0002, South Africa*

[2]*Physics Department, Shendi University, Shendi, Sudan*

[3]*Joint Institute for Nuclear Research, Dubna, Russia*

[4]*Department of Physics, Nelson Mandela University (NMU), , Port Elizabeth, South Africa*

[5]*Centre for HRTEM, Nelson Mandela Metropolitan University, Port Elizabeth, South Africa*

*Corresponding author: Thulani.Hlatshwayo@up.ac.za

## ABSTRACT

Silver (Ag) ions of 360 keV were implanted into polycrystalline SiC to a fluence of $2\times10^{16}$ cm$^{-2}$ at room temperature. Some of the as-implanted samples were irradiated with xenon (Xe) ions of 167 MeV to a fluence of $3.4\times10^{14}$ cm$^{-2}$ at room temperature. After implantation, the un-irradiated and irradiated samples were isochronally annealed at temperatures ranging from 1100 to 1500 °C in steps of 100 °C for 5 hours. The as-implanted, irradiated and annealed samples were characterized by Rutherford backscattering spectrometry (RBS), Raman spectroscopy, transmission electron microscopy (TEM) and scanning electron microscopy (SEM). Implantation of Ag at room temperature amorphized the SiC near surface implanted region, while swift heavy ion (SHI) irradiation of the as-implanted samples caused some limited recrystallization of the amorphized layer. Migration of implanted Ag was already taking place at 1100 °C in the irradiated samples while no Ag migrate for the un-irradiated sample annealed at the same temperature. These difference in the migration behavior of Ag is due to the difference in microstructure in the two samples. Irradiated samples had fine crystals with the presence of pores in the surface after annealing at 1100 °C. The pores led to the loss of about 70% of Ag from the surface. While un-irradiated samples had relatively larger crystals with less loss of silver. Decomposition of SiC were observed after annealing at 1500 °C in both samples. The results show that more Ag was released in the irradiated SiC samples.

**Keywords**: SHI, RBS, SiC, Structure.

## 1. Introduction

The triple coated isotropic (TRISO) particle is a robust fuel form designed for use in high temperature gas-cooled reactors (HTGRs) [1-4]. This particle consists of a small round $UO_2$ kernel encapsulated with four chemical vapour deposited (CVD) layers [5]. The first layer is a porous carbon buffer. This layer reduces recoiling fission products (FPs) and accommodates internal gas buildup. The other three layers are the inner pyrolytic carbon (IPyC) layer that acts as a diffusion barrier to most non-metallic FPs, a silicon carbide (SiC) layer that acts as a main diffusion barrier to FPs and an outer pyrolytic carbon (OPyC) layer that protects SiC. SiC can exist in different forms of more than 200 polytypes depending on the stacking sequence [6]. When fabricated by the CVD, it is commonly found as 3C, 4H, 6H and 15R [7]. Current TRISO design use the CVD method for growing polycrystalline SiC in such a way that the crystallites are predominantly 3C which is preferred polytype for high temperature nuclear reactor applications [6,8-9]. TRISO particles retain most of the radiological important FPs with the exception of strontium (Sr), Europium (Eu) and silver ($^{110m}$Ag) [10]. $^{110m}$Ag is a strong gamma emitter with relative longer half-life of about 253 days [11]. This makes silver to be one of the key FPs whose transport properties in the TRISO particle need to be investigated. For over four decades, scientists have investigated the migration behavior of Ag in the SiC. Extensive studies have been performed to explain the transport mechanism of Ag, including out-of-pile release measurements from irradiated TRISO fuel [12-15], and ion implantation to investigate silver behavior in SiC at higher temperature [16-19]. One of the properties of 6H (α) and 3C (β) silicon carbide is that it is can be easily amorphized by ion implantation at or below room temperature [20-24].

A fission reaction occurs (in the kernel inside TRISO particle) when a uranium nucleus absorbs a slow neutron. The uranium nucleus then becomes unstable and split into smaller nuclei, releasing different energies including energies in the order of 100 MeV i.e. the energy range of swift heavy ions (SHIs) and two or three neutrons. These ions lose most of their energies firstly via electron excitations and later nuclear stopping.

The energy loss of SHIs as they traverse through SiC layer can cause changes in the structure of SiC. The structural changes in SiC (i.e phase transition and

amorphous latent track formation) by SHIs were not observed even up to the practical upper limit of electronic stopping power for SiC, Se = 34 keV/nm [25,26]. At the same time, it was found that the recrystallization of an initially damaged /amorphous polycrystalline SiC layer resulting in randomly orientated nanocrystallites after SHIs irradiation at room temperature and 500 °C [27,28]. To explain the results the thermal spike model was proposed [29]. These structural changes by SHIs might influence the migration behavior of FPs in SiC. As extensively reviewed in [3,30] the microstructure of SiC can affect the migration behavior of Ag. Recently, few studies have investigated the migration behavior of different FPs in SiC after SHIs irradiation. No migration of implanted I, Kr and Xe in SiC has been detected after SHI irradiation at room temperature and at 500 °C [27,28,31]. Apart from the effect of carbon ions irradiated in Ag implanted SiC, no other post SHI irradiation annealing results have been reported [32].

As mentioned above and extensively reviewed in [3], high fluence (~ $10^{16}$ $cm^{-2}$) ion bombardment at room temperature causes amorphization of the implanted layer in SiC, either in single crystalline or polycrystalline SiC. Recrystallization into a polycrystalline structure starts to occur after annealing at 800 °C [3,33]. One of the advantages of SiC is its radiation hardness at elevated temperatures, that is, it cannot be amorphized by ion bombardment at substrate temperatures above 350 °C and remains crystalline [34]. For neutron irradiation this critical temperature for amorphization is about 150 °C [6,35]. Since the SiC layer in the TRISO fuel particles is the main diffusion barrier for fission products [5], these relatively low critical temperatures for amorphization are an advantage for the TRISO particles. TRISO fuel particles will be used in the generation IV nuclear reactors, such as the Pebble Bed Modular Reactor (PBMR) [4]. These reactors will operate at high temperatures, i.e. above 600 °C, allowing the SiC layer to remain crystalline, albeit with defects introduced by the neutron bombardment.

The purpose of this paper was two-fold. It was first to investigate structural changes in room temperature Ag implanted polycrystalline SiC after SHI irradiation at room temperature. Raman spectroscopy was used to study the microstructure of both sets of samples before and after vacuum annealing at temperatures between 1100 and 1500 °C. Scanning electron microscopy was used to determine morphological changes after these treatments. Although the migration of silver in SiC has been

thoroughly investigated over several decades, there have been very few ones on the effect of SHI on this migration. It is known that SHI irradiation affects the microstructure of the substrate. The latter can again affect the diffusion behaviour. Consequently, the paper also qualitatively investigates the migration behaviour of Ag in SHI irradiated and un-irradiated samples. For this purpose Rutherford backscattering spectrometry was used.

## 2. Experimental Method

In this study, the polycrystalline CVD-SiC wafers from Valley Design Corporation were used. For a previous study [16] the as-received samples were characterized by electron backscatter diffraction (EBSD) and were found to be composed mainly of 3C-SiC crystallites, but with some hexagonal phases also present. Since EBSD is only a surface technique, the samples were also investigated by X-ray diffraction in the present study to determine the crystal composition of the bulk. XRD spectra (not shown) confirmed the EBSD results that the samples were mainly cubic SiC (3C-SiC) with a small peak belonging to hexagonal SiC.

The as-received samples were implanted with 360 keV $Ag^+$ ions to a fluence of $2\times10^{16}$ $cm^{-2}$ in vacuum at room temperature at the Friedrich-Schiller-University Jena, Germany. The implantation was performed at room temperature in order to amorphize the implanted layer. This was done to compare the migration behavior of Ag in the initially amorphous SiC (in the as-implanted) and in the amorphous SiC after SHI irradiation.

Some of the implanted samples were irradiated with 167 MeV $Xe^{+26}$ ions to a fluence of $3.4\times10^{14}$ $cm^{-2}$ in vacuum at room temperature using the IC-100 FLNR cyclotron in JINR, Dubna, Russia.

Irradiated and un-irradiated samples were subjected to isochronal annealing for 5 hours using a high vacuum computer-controlled *Webb 77* graphite furnace. The migration behaviour of implanted Ag in both samples was investigated using annealing temperatures ranging from 1100 to 1500 $^{o}C$ in steps of 100 $^{o}C$. The as-implanted, implanted then irradiated and annealed samples were characterized by Raman spectroscopy, transmission electron microscopy (TEM), scanning electron microscopy (SEM) and Rutherford backscattering spectrometry (RBS). Raman

analyses was recorded using a T64000 series II triple spectrometer system from HORIBA Scientific, Jobin Yvon Technology. The 514.3 nm laser line of a coherent Innova® 70C series $Ar^+$ laser (spot size ~ 2 μm) with a resolution of 2 $cm^{-1}$ in the range of 200 $cm^{-1}$ – 1800 $cm^{-1}$ was used. The measurements were obtained in a backscattering configuration with an Olympus microscope attached to the instrument (using an LD 50x objective). The laser power was set at 1.7 mW. An integrated triple spectrometer was used in the double subtractive mode to reject Rayleigh scattering and dispersed the light onto a liquid nitrogen cooled Symphony CCD detector. The Raman spectra were recorded under these conditions and normalized to have the same scale. Cross-sectional TEM specimens were prepared using an FEI Helios Nanolab 650 FIB. Thinning of the specimens were performed by successive 30 keV and 5 keV Ga ions. Final polishing was done at 2 keV. TEM specimens were analysed using a JEOL JEM 2100 LAB6 transmission electron microscope operating at 200 kV. SEM was performed using a high-resolution Zeiss Ultra Plus 55 field emission scanning electron microscopy (FESEM) operated at 2 kV under vacuum. The changes in the Ag profiles on irradiated and un-irradiated samples before and after annealing were monitored by RBS using $He^+$ ions of 1.6 MeV. The backscattered $He^+$ ions were detected using a silicon surface barrier detector set at a 165° and charge of 8 μC was collected per measurement. The RBS Ag profiles in energy channels were converted into depth using energy loss data and the density of SiC (3.21 $gcm^{-3}$).

## 3. Results and discussion

Fig.1 (a) shows the SRIM 2010 [36] simulation of the implanted Ag depth profile into SiC and displacement per atom (dpa) caused by 360 keV Ag ion implantation and Fig. 1 (b) shows the Xe depth profile with displacement per atom (dpa) caused by 167 MeV Xe ions irradiation. Displacement energies of 35 and 20 eV for Si and C respectively were used in the simulation [37]. If one assumes the minimum dpa to cause amorphization SiC is 0.3 dpa [38], it is quite clear that implantation of Ag will result in the amorphous layer of about 160 nm and Xe ions do not amorphize SiC. From Figure 1 (a) there is also evidence of Ag ions and damage deeper than those resulting from the "normal" implantation of 360 keV Ag ions. These are probably due to knock-on effects. From these results, it is quite clear that the as-implanted Ag will be embedded in the amorphous region and this region will be extensively exposed to

large amounts of energy deposition due to electronic energy loss of the penetrating ions.

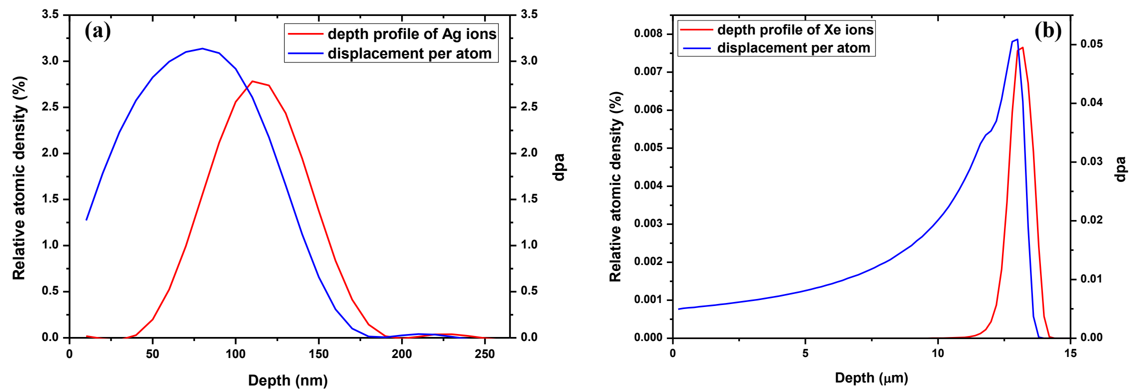


***Fig. 1***: *Simulated depth profiles and displacement per atom (dpa) obtained using SRIM 2010 [36], (a) Ag depth profile and displacement per atom (b) Xe depth profile and displacement per atom.*

Raman spectra of the un-implanted (virgin), as-implanted and irradiated samples are shown in Fig. 2. The Raman spectrum of un-implanted SiC shows the characteristic Raman peaks of SiC [27]. Implantation of Ag into SiC at room temperature resulted in the disappearance of characteristic SiC Raman peaks between 600 to 1000 $cm^{-1}$ and appearance of broad peak of Si-Si vibrations at around 510 $cm^{-1}$. This was accompanied by the damaged SiC band at around 800 $cm^{-1}$ and C-C vibrations around 1425 $cm^{-1}$. These changes indicate the amorphization of SiC layer after implantation.

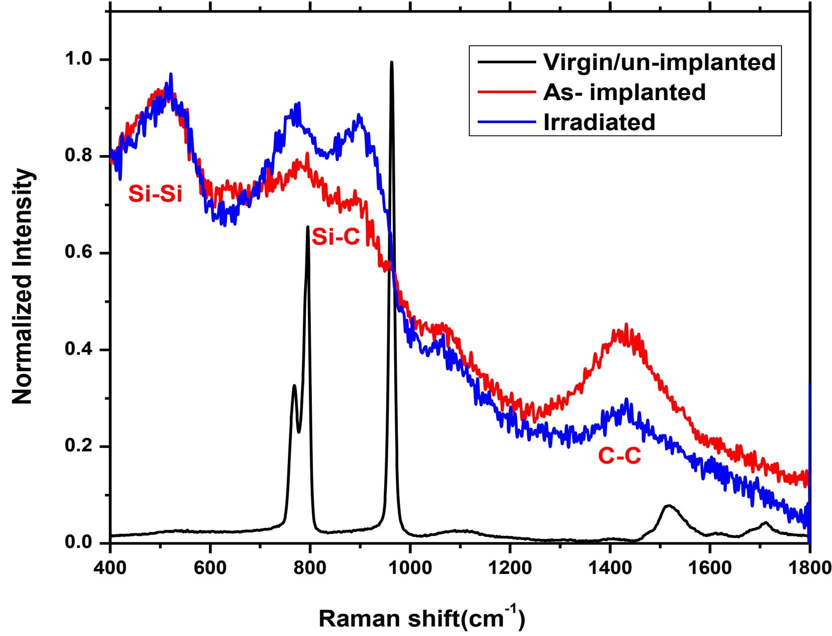


***Fig. 2**: Raman spectra of the virgin SiC (virgin), implanted with 360 keV Ag ions (as-implanted), implanted with Ag then irradiated with 167 MeV Xe ions to a fluence of $3.4\times10^{14}$ $cm^{-2}$ (Irradiated).*

Irradiation of implanted SiC with Xe (167 MeV) ions at room temperature to a fluence of $3.4\times10^{14}$ $cm^{-2}$ caused the reappearance of broad SiC Raman characteristic peaks at around 770 and 895 $cm^{-1}$ with the Si-Si (around 525 $cm^{-1}$) and C-C (around 1433 $cm^{-1}$) peaks still present. The appearance of broader characteristic SiC peaks indicates some recrystallization of the initially amorphous SiC layer. Similar recrystallization of SiC implanted with different implanted ions after SHIs irradiation has been reported previously [27,28]. In these previous studies, the recrystallization was found to be due to SHIs irradiation causing the formation of randomly oriented crystallites embedded in amorphous SiC.

Fig. 3 (a) and (b) shows TEM micrographs of Ag implanted SiC un-irradiated and irradiated by Xe ions of 167 MeV at room temperature to a fluence of $3.4\times10^{14}$ $cm^{-2}$, respectively. Arrows in Fig. 3 indicate the implantation and irradiated direction; the circles indicate where the damage regions and where the selected area diffraction (SAD) patterns were taken. The SAD pattern of the as-implanted region showed a diffused ring indicating the amorphisation of SiC, while the diffused ring was replaced by defined ordered pattern in the implanted and then irradiated samples. The latter suggests some recrystallization after irradiation. Amorphisation of SiC after silver

implantation (360 keV) to fluence of $2\times10^{16}$ $cm^{-2}$ at RT has been observed [16] and some recrystallization of the initial amorphised SiC after swift heavy ions irradiation has been recently reported [27, 28]. Comparing the present results with results reported in [27, 28], recrystallization seems to be enhanced in the silver implanted samples.

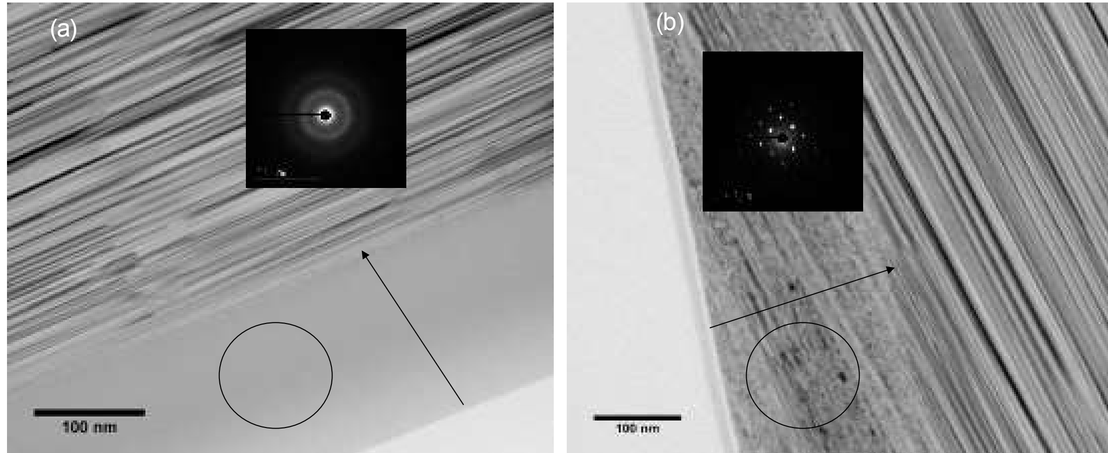


***Fig. 3:*** *TEM micrograph of polycrystalline SiC implanted with Ag to a fluence of $2\times10^{16}$ $cm^{-2}$ at room temperature (a) and subsequently irradiated with Xe (167 MeV) at a fluence of $3.4\times10^{14}$ $cm^{-2}$ (b).*

The SEM micrographs of the as-received/virgin, as-implanted and irradiated samples are shown in Fig. 4. The SEM image of the as-received sample showed polishing marks_(Fig. 4 (a) and (a')), which disappeared after implantation at room temperature as seen in Fig. 4 (b) and (b'), confirming the amorphization of SiC as revealed by SRIM, Raman and TEM results. Irradiating the Ag implanted samples at room temperature to a fluence of $3.4\times10^{14}$ $cm^{-2}$ shows no major changes in the samples surface as compared to the as-implanted-Fig. 4 (c) and (c'). The lack of changes in the irradiated implies that the resulting changes on the surface are below the SEM detection limit.

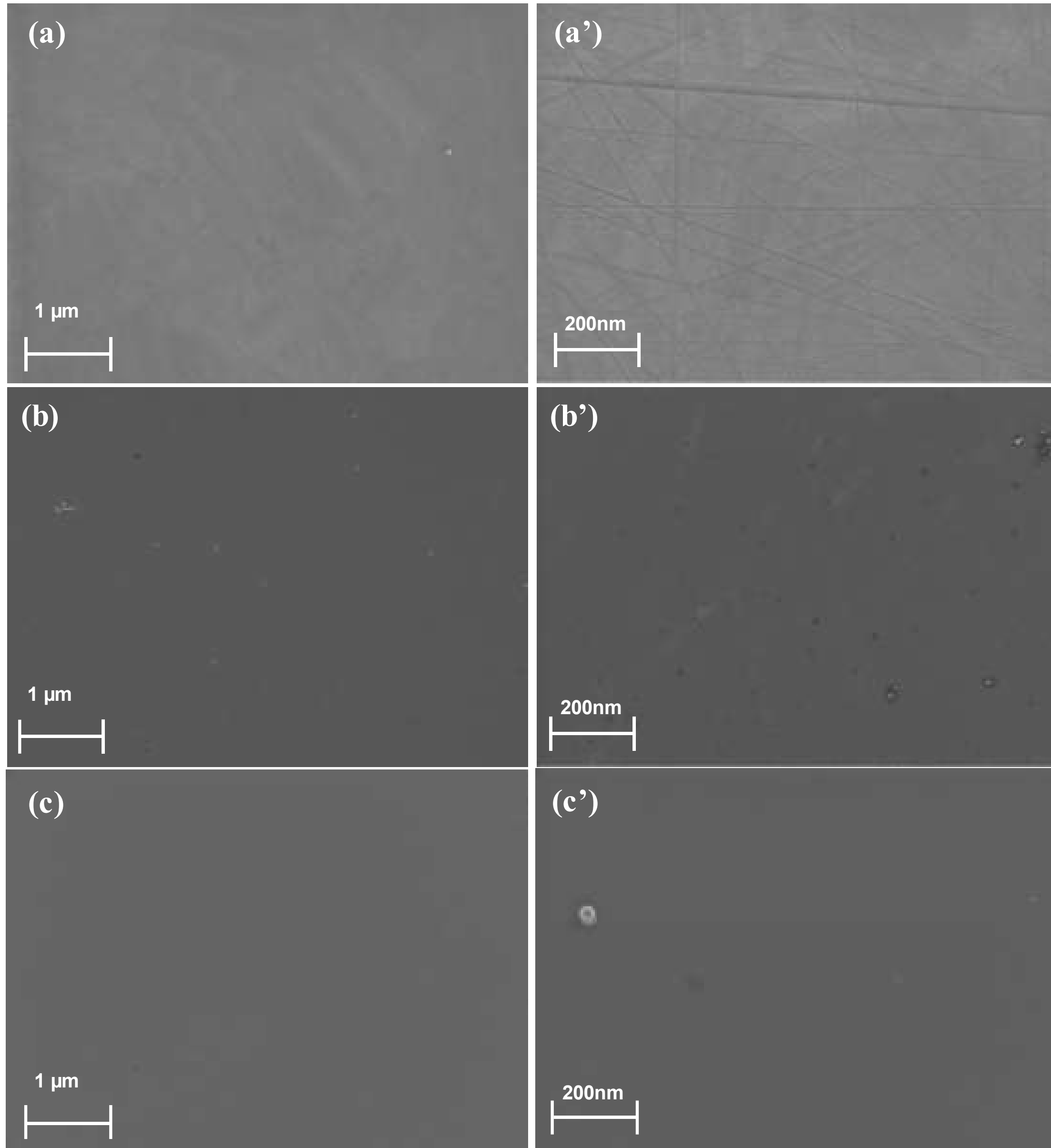


***Fig. 4****: SEM micrographs of the CVD-SiC surface (a), (b) and (c) low magnification of as-received, as-implanted with Ag and implanted with Ag then irradiated with Xe ions at room temperature to a fluence of $3.4\times10^{14}$ cm$^{-2}$, respectively. (a'), (b') and (c') high magnification for (a), (b) and (c) images, respectively.*

The un-irradiated and irradiated samples were sequential annealed from 1100 to 1500 °C. Raman spectra of both samples at 1100 °C are shown in Fig. 5. Both samples showed the reappearance of the characteristic peaks of SiC. The un-irradiated sample showed full recrystallization resulting in the appearance of Raman characteristic peaks of SiC. The irradiated sample showed poor recrystallization with a broad Si-Si peak at about 545 cm$^{-1}$, the C-C peak at 1520 cm$^{-1}$, and the LO and TO characteristic peaks of SiC which appeared in the same position as the un-irradiated

sample. The LO mode SiC for the un-irradiated sample at about 960 $cm^{-1}$ had a slightly higher intensity compared to that of the SHI irradiated sample. This suggests that the un-irradiated sample has larger crystals compared to the irradiated sample. These observations are in agreement with a previous study [39], which showed that the LO mode property is strongly crystal size dependent. These variations in Raman intensities were accompanied by an increase in the FWHM of the SiC Raman prominent peak (around 960 $cm^{-1}$) from 9.4 $cm^{-1}$ (virgin) to 10.6 $cm^{-1}$ and 14.5 $cm^{-1}$ for un-irradiated and irradiated samples respectively. The FWHM of the un-irradiated samples was narrower compared to the irradiated samples. This confirms that annealing the un-irradiated samples at 1100 °C resulted in larger crystallites compared to irradiated samples annealed in the same conditions [40]. This is rather surprising, as the irradiated samples had randomly oriented crystallites embedded in the amorphous SiC while the un-irradiated was fully amorphous. Therefore, the recrystallization in these samples are different. This might be due to the difference in impurity concentrations in both samples. The impurity can be Ag. The different Ag concentrations will be explained later in the paper when we discuss the RBS results. In general, impurities can usually retard recrystallization process and inhibit crystal growth [41,42].

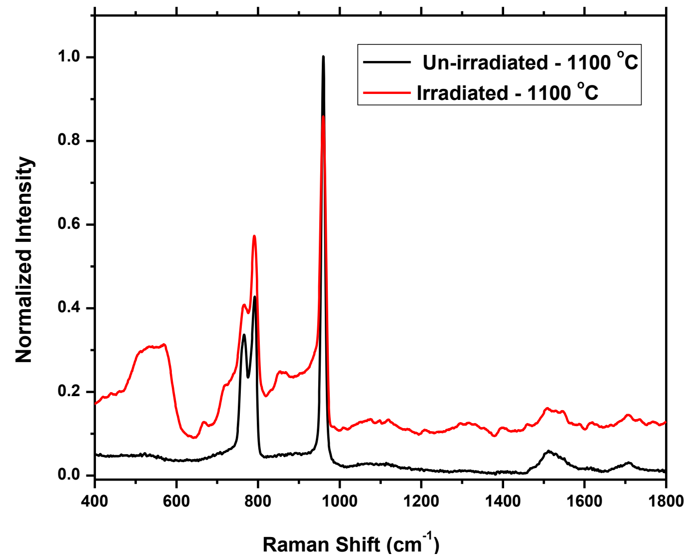


***Fig. 5**: Raman spectra of SiC implanted with Ag at room temperature then annealed at 1100 °C (un-irradiated - 1100 °C), implanted and then irradiated with Xe ions to fluences of $3.4\times10^{14}$ $cm^{-2}$ and annealed at 1100 °C (irradiated-1100 °C).*

The crystallization observed by Raman spectroscopy in Fig. 5 was also evident in the SEM images shown in Fig. 6. After implantation the surfaces were featureless, as is typical of bombardment induced amorphous SiC layers. As can be seen from Fig. 6 (a) and (a'), annealing of the un-irradiated samples resulted in the long thin crystals growing in random directions. However, it shows also smaller crystals present on the surface. The surfaces of irradiated samples (Fig. 6 (b) and (b')) had a fine crystals SiC layer after annealing at 1100 °C with many pores appearing on their surfaces. Comparison between these findings with the Raman results clearly shows a difference in the recrystallization between un-irradiated and irradiated samples. Apart from the influence of impurities as discussed above, this difference in the recrystallization might also be due to the fact that the initial surfaces/layers were in different states before annealing, i.e. the un-irradiated samples were amorphous while the irradiated samples were composed of crystallites that were randomly orientated in an amorphous matrix.

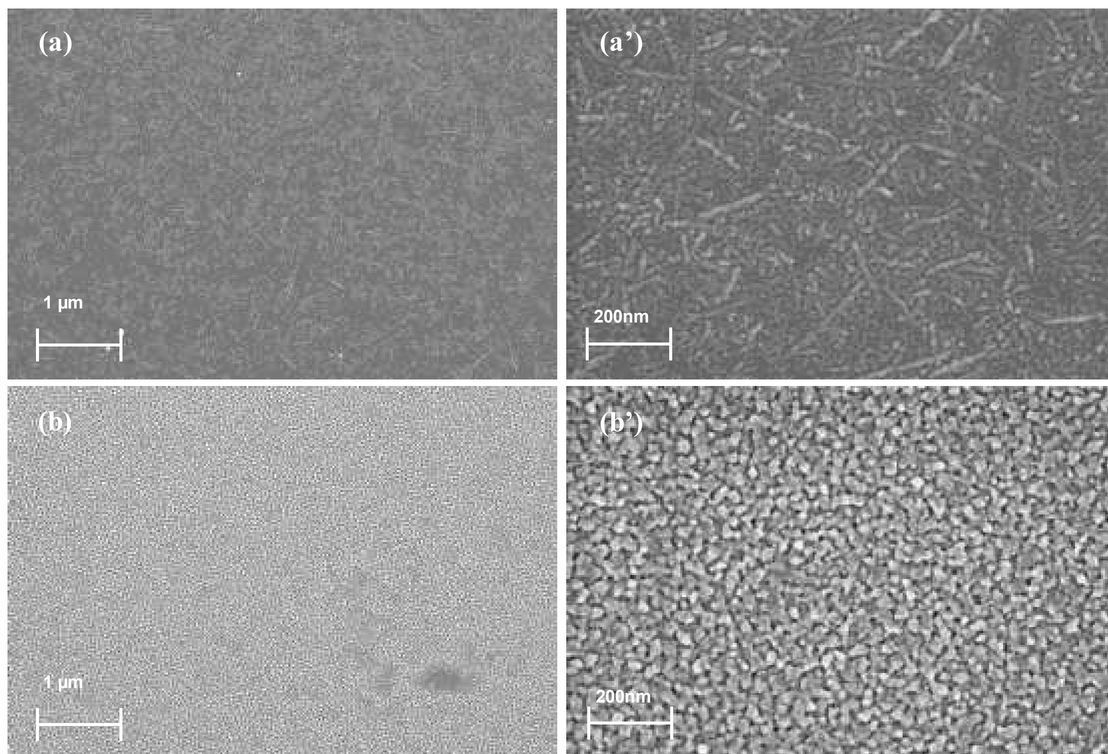


***Fig. 6****: SEM micrographs of samples annealed at 1100 °C. (a) and (b) low magnification of un-irradiated and irradiated with Xe to a fluence of $3.4\times10^{14}$ cm$^{-2}$, respectively. (a') and (b') high magnification for (a) and (b) un-irradiated and irradiated sample, respectively.*

Raman spectra of the as-implanted and irradiated samples after sequentially annealing up to 1500 °C are shown in Fig. 7. In both the un-irradiated and irradiated

samples peaks at 1350 and 1580 $cm^{-1}$ appeared corresponding to D and G peaks respectively. This indicates the presence of a carbon layer on the sample surfaces after annealing at 1500 $^{o}C$. These carbon peaks were not observed after annealing at temperatures from 1200 to 1400 $^{o}C$.

The SEM micrographs of both irradiated and un-irradiated samples after sequentially annealing up to 1500 $^{o}C$ are shown in Fig. 8. Both samples maintained their initial main surface features observed at lower temperatures i.e. the un-irradiated was composed of larger crystals while the irradiated was composed of finer crystals. A comparison between Figures 6(b') and 8(b') shows that the crystallites have increased in size with the increase in temperature. The increase in temperature increases the mobility of atoms leading to the increase in average crystal size, in line with crystal growth theory [41,42]. Some of the crystallites were protruding more than others. Obviously, this effect was more visible on the un-irradiated samples with their larger crystals. This can be explained in terms of Wulff's law (i.e. the preferential growth of a crystal surface with a lower surface energy compared to another surface with a higher surface energy) [43,44]. In addition, thermal etching can play a contributing role at this temperature for both samples [44]. As can be seen from Fig. 8 (b) and (b'), the surface morphology of the irradiated sample after annealing at 1500 °C did not change significantly from those annealed at lower temperatures. Apart from the crystallites being slightly larger, very few and only small pores were visible. In contrast, these pores were larger and clearly visible in samples annealed at 1100 °C - see Fig 6(b'). The same explanations for crystal growth as used above are applicable here. Fig 8(a) and (a') shows thin strands of carbon material between the SiC crystallites and clusters with few and very small pores on the surface after annealing at 1500 °C.

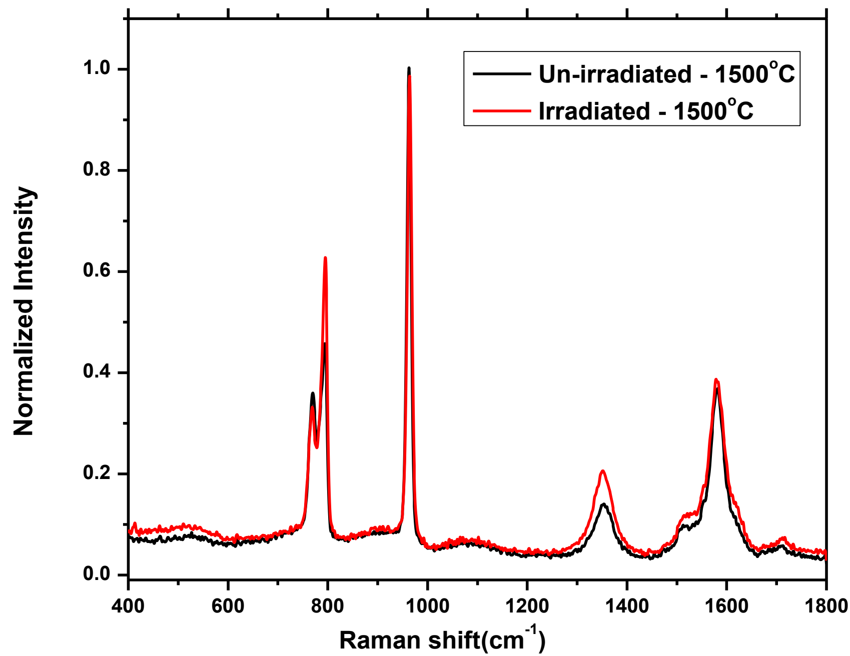


***Fig.** 7: Raman spectra of SiC implanted with Ag at room temperature and then sequentially annealed up to 1500 °C (Un-irradiated -1500 °C), implanted and then irradiated to fluences of $3.4\times10^{14}$ $cm^{-2}$ and sequentially annealed up to 1500 °C (Irradiated – 1500 °C).*

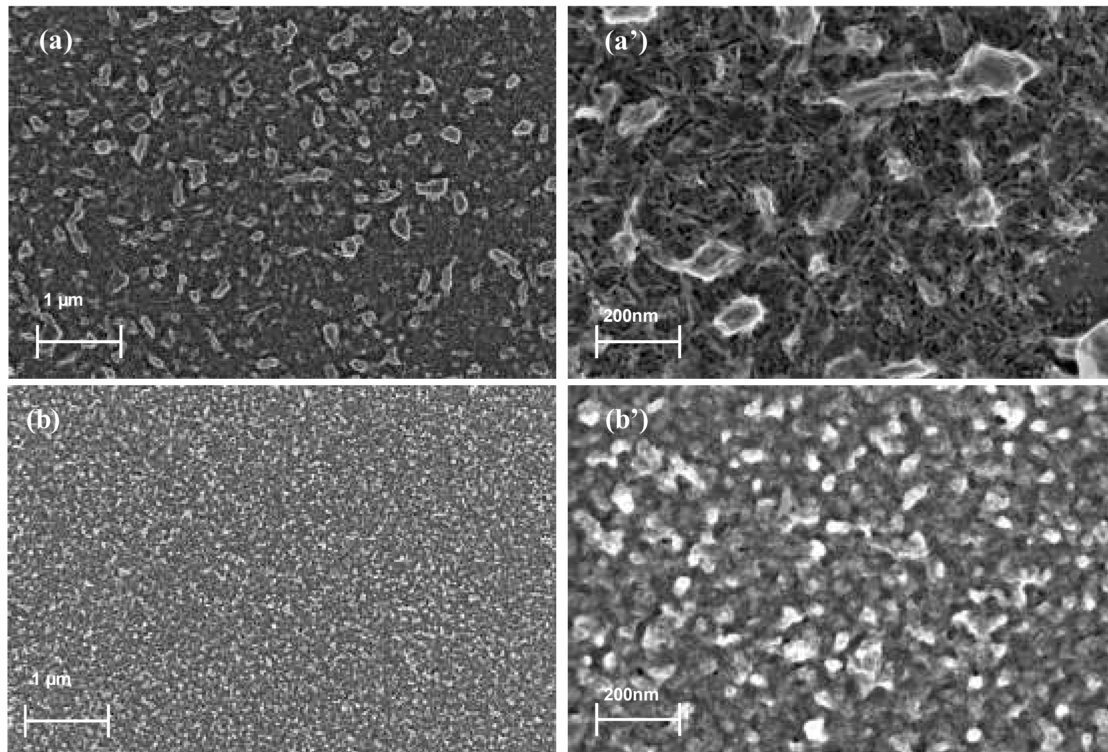


***Fig.** 8: SEM micrographs of irradiated and un-irradiated samples after sequentially annealing up to 1500 °C (a) and (b) low magnification of un-irradiated and irradiated with Xe ions to a fluence of $3.4\times10^{14}$ $cm^{-2}$, respectively. (a') and (b') high magnification for (a) and (b) un-irradiated and irradiated sample, respectively.*

Fig. 9 shows the RBS spectra of SiC (both un-irradiated and irradiated samples) after sequentially annealing from 1100 to 1500 ºC for 5 hours in steps of 100 ºC. The Ag peaks are not shown in the two spectra. Arrows in Fig. 9 indicate the Si and C surface channel positions. Spectra look the same before and after implantation, irradiation and annealing from 1100 to 1400 ºC. Annealing these samples at 1500 ºC resulted in the accumulation of carbon on the SiC sample surface. This was accompanied by the shift of the Si surface energy channel positions to lower energy channel positions indicating the presence of a carbon layer on the SiC surfaces. The free carbon on the surfaces was due to thermal decomposition of SiC causing the sublimation of silicon thus leaving a free carbon layer on the surface. The decomposition of implanted SiC layers has been reported previously [16,18,44] to occur at temperatures above 1400 °C. The decomposition of SiC observed in RBS at 1500 ºC correlates with Raman results (Fig. 7) which showed the appearance of the D and G peaks at this temperature and with the SEM image shown in Fig. 8 (a) and (a').

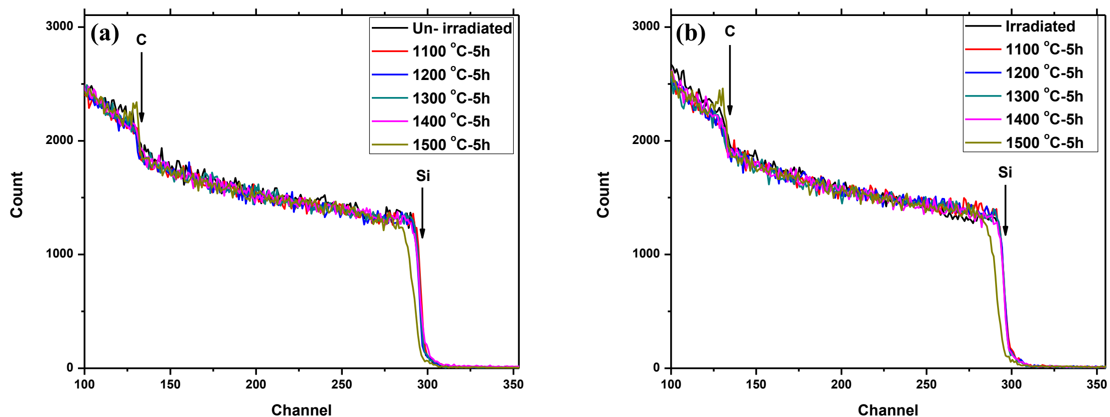


***Fig. 9:*** *SiC RBS spectra of irradiated and un-irradiated samples before and after sequentially annealing up to 1500 ºC. (a) Un-irradiated, (b) Implanted with Ag then irradiation with Xe at room temperature to a fluence of* $3.4\times10^{14}$ *cm*$^{-2}$*.*

Migration behaviour of Ag implanted into SiC was investigated after irradiation and sequential annealing. SHIs irradiation of the implanted samples did not result in any detectable change in the implanted Ag profile indicating no migration of implanted Ag as can be seen from Fig. 10. The lack of migration of the implants after SHIs irradiation at room temperature has been reported for other fission products surrogates [27,28].

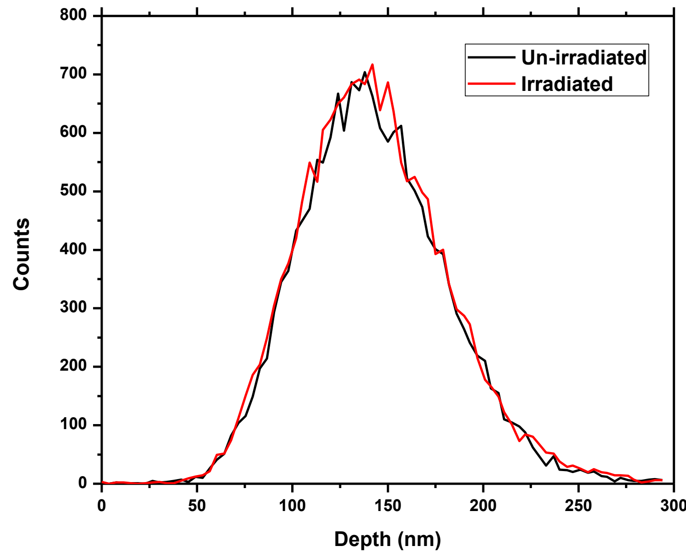


***Fig. 10:*** *Ag depth profile from un-irradiated and irradiated samples.*

Silver depth profiles of irradiated and un-irradiated samples after sequential annealing at temperatures ranging from 1100 to 1500 °C for 5 hours are shown in Fig. 11. From Fig. 12 it follows that annealing the SHI irradiated samples at 1100 °C resulted in significant loss (of about 70%) of implanted Ag. This was due to the presence of pores in the surface extending into the implanted layer - Fig. 6(b’). This observation is in agreement with previous studies [18,45], which showed that implanted Ag sublimated via pores into the vacuum during annealing. The different amounts of retained silver after annealing were due to the difference in surface morphology of the samples. It has been reported that Ag somehow enhances the recrystallization of initial amorphized SiC [46]. As mentioned above, the growth of the crystallites led to the closure of the pores though which the sublimated Ag can escape into the vacuum. No further loss of Ag was observed in the irradiated sample after annealing at temperatures from 1200 to 1400 °C. This was due to very small pores as showed in Fig. 13 (b’), (d’) and (f’), compared to the irradiated sample annealed at 1100 °C in Fig. 6(b’). This reduction of pores size is due to the grain growth of SiC crystals. The Ag peak shifted towards the surface after annealing at 1400 °C, probably due to thermal etching [18]. Further loss of implanted silver accompanied by a shift towards the surface was observed after annealing at 1500 °C. This shift is due to the thermal etching of SiC that increases exponentially at 1500 °C [44].

Slight migration of implanted Ag (see Fig. 11(a)), accompanied by a slightly loss of Ag (see Fig. 12) were observed after annealing at 1100 °C for un-irradiated samples. After annealing at 1200 °C, the Ag profile of the un-irradiated sample broadened and there was loss of about 6% of the Ag. Such symmetric broadening of an implanted species is characteristic of Fickian diffusion [47]. This broadening became more pronounced at 1300 °C and about 12% of implanted Ag was lost. At 1400 °C, Ag profile peak shift towards the surface (similar to the irradiated sample) due to thermal etching. More than 76% of Ag was lost after annealing at 1500 °C due to the pores on the surface and thermal etching. The Ag profile peak further shifted towards the surface, which caused an asymmetric peak.

The small loss of Ag in the un-irradiated samples and the high loss of Ag in the irradiated samples after annealing at 1100 °C were due to different structures in the annealed un-irradiated and irradiated samples. Annealing the un-irradiated samples at this temperature led to the formation of rather large crystals while annealing the irradiated samples produced fine crystal structures with the presence of pores. This resulted in high amount of Ag released in the latter samples. From these results, it is quite clear that Ag releasing is favored in the irradiated SiC structure.

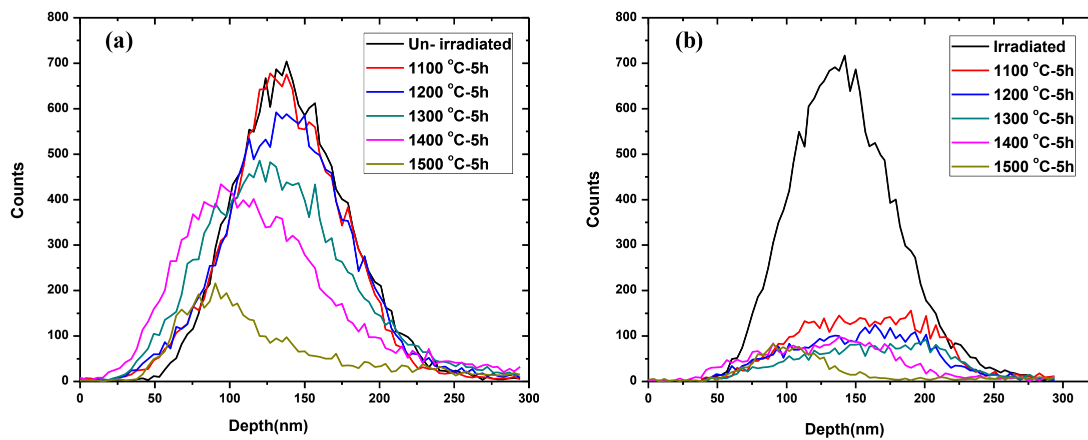


***Fig. 11:*** *RBS Ag depth profiles for irradiated and un-irradiated samples before and after annealing. (a) Ag depth profiles for un-irradiated samples. (b) Ag depth profiles for irradiated samples with Xe at room temperature to a fluence of* $3.4\times10^{14}$ $cm^{-2}$.

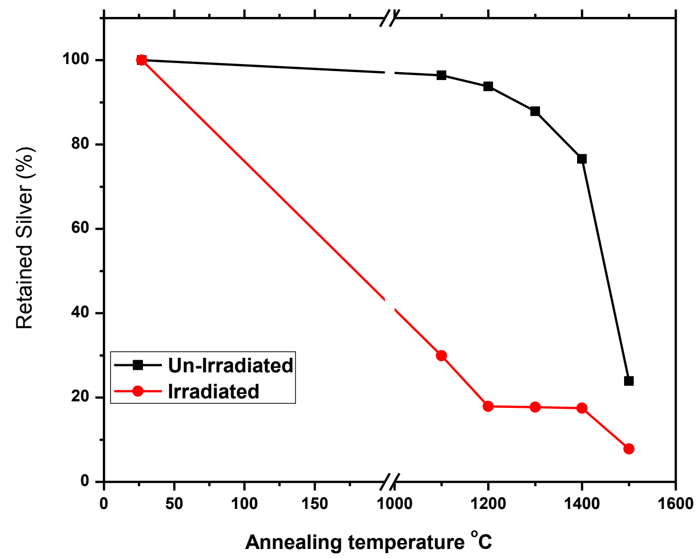


***Fig. 12:*** *The retained ratio of silver in irradiated and un-irradiated samples before and after sequential annealing up to 1500 $^{0}$C.*

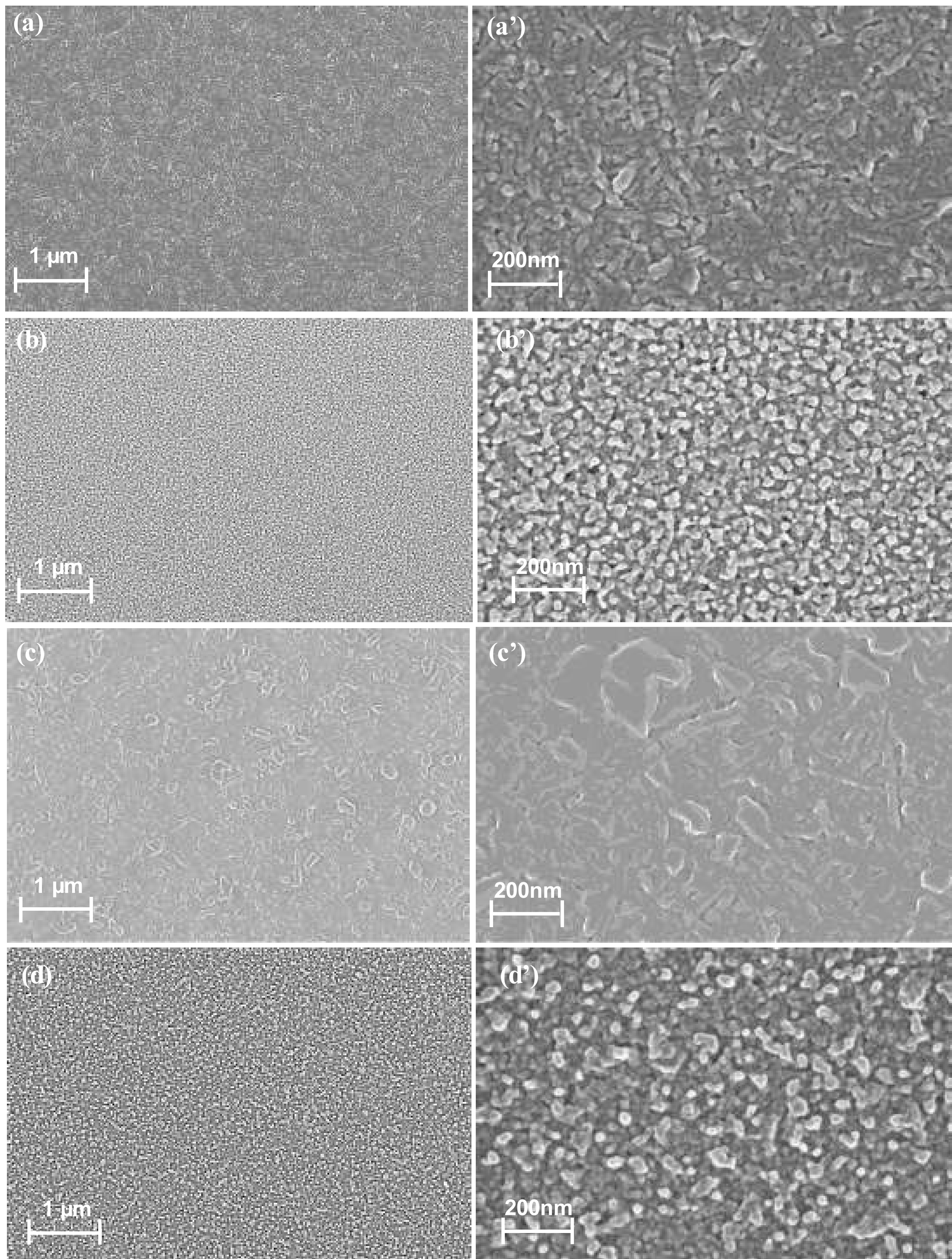
(a)
1 µm
(a')
200nm
(b)
1 µm
(b')
200nm
(c)
1 µm
(c')
200nm
(d)
1 µm
(d')
200nm

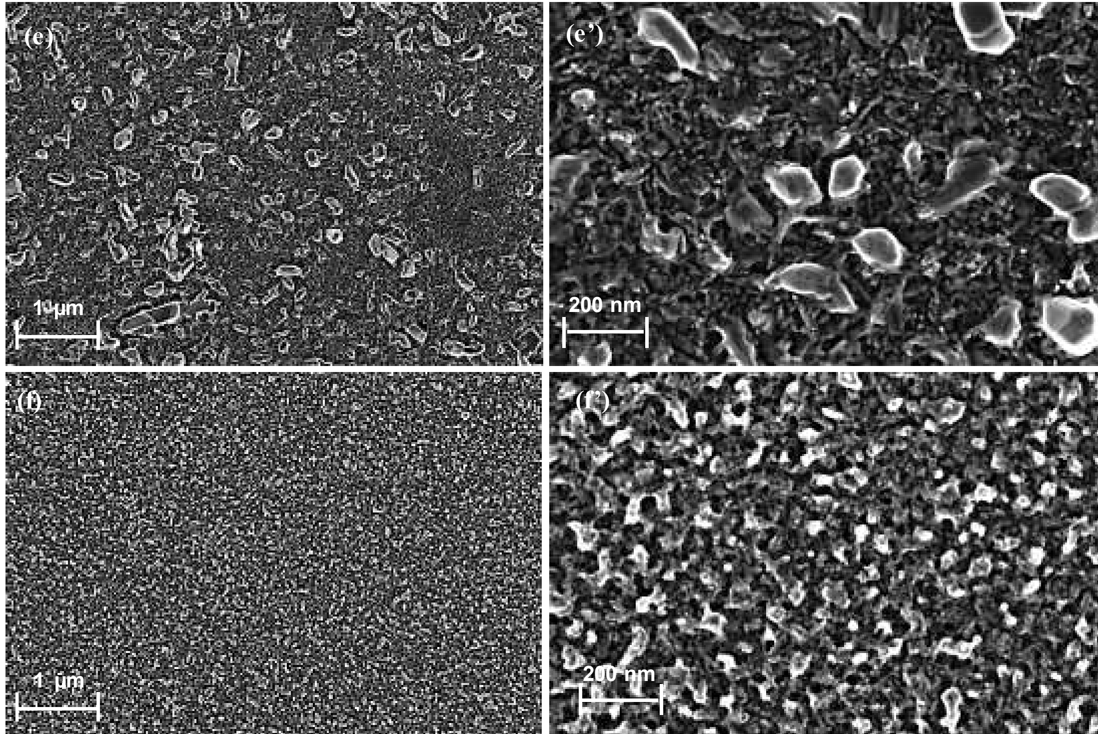


***Fig. 13:*** *SEM micrographs of samples sequentially annealed at 1200 °C, 1300 °C and 1400 °C. (a), (c) and (e) low magnification of un-irradiated samples annealed at 1200 °C, 1300 °C and 1400 °C respectively. (a'), (c') and (d') high magnification for (a), (c) and (e) images, respectively. (b), (d) and (f) low magnification of irradiated samples annealed at 1200 °C, 1300 °C and 1400 °C respectively. (b'), (d') and (f') high magnification for (b), (d) and (f) images, respectively.*

## 4. Conclusion

The influence of SHIs irradiation on the migration behavior of Ag implanted in polycrystalline SiC have been investigated using RBS, Raman, TEM and SEM. The as-implanted and SHIs irradiated samples were vacuum annealed at 1100 to 1500 °C in steps of 100 °C for 5 hours. Implantation of silver amorphized the SiC, while SHIs irradiation of the as-implanted SiC resulted in limited recrystallization of the initially amorphized SiC. Annealing at 1100 °C already caused recrystallization in both un-irradiated and irradiated samples. At 1500 °C, a carbon layer appeared on the surface of the both samples, this was due to the sublimation of silicon leaving a free carbon layer on the surface.

SHIs irradiation alone did not induce any measurable migration of the implanted Ag. However, annealing the samples at 1100 °C caused strong releasing of implanted silver in SHIs irradiated samples with slight releasing in un-irradiated

samples. The enhanced Ag releasing in SHIs irradiated samples was explained in terms of the high number of pores in the irradiated samples compared few pores in the un-irradiated samples. The results show that more Ag was released in the irradiated SiC samples.

## 5. References


[1] D.A. Petti, P.A. Demkowicz, J.T. Maki, R.R. Hobbins, TRISO-Coated particle fuel performance, Compr. Nucl. Mater. 3 (2012) 151–213.

[2] K. Verfondern, H. Nabielek, J.M. Kendall, Coated particle fuel for high Temperature gas cooled reactors, Nucl.Eng. Des. 39(2007) 603–616.

[3] J.B. Malherbe, Topical Review: Diffusion of fission products and radiation damage in SiC, J. Phys. D Appl. Phys. 46 (2013) 473001 (27 page).

[4] J.B. Malherbe, E. Friedland, N.G. van der Berg, Ion beam analysis of materials in the PBMR reactor, Nucl. Instrum. Methods Phys. Res. B 266 (2008) 1373-1377.

[5] N. G. van der Berg, J. B. Malherbe, A. J. Botha and E. Friedland, SEM analysis of the microstructure of the layers in triple-coated isotropic (TRISO) particles, Surf. Interface Anal. 42 (2010) 1156–1159.

[6] L.L. Snead, T. Nozawa, Y. Katoh, T.-S. Byun, S. Kondo, D.A. Petti, Handbook of SiC properties for fuel performance modeling, J. Nucl. Mater. 371 (2007) 329-377.

[7] H. Abderrazak, E. S. Bel Hadj, R. Gerhardt (Ed.), Silicon carbide: synthesis and properties, properties and applications of silicon carbide, InTech, (2011). DOI: 10.5772/15736. Available from: https://mts.intechopen.com/books/properties-and-applications-of-silicon-carbide/silicon-carbide-synthesis-and-properties.

[8] E. Lopez-Honorato, C. Brigden, R.A. Shatwell, H. Zhang, I. Farnan, P. Xiao, P. Guillermier, J. Somers, Silicon carbide polytype characterisation in coated fuel particles by Raman spectroscopy and $^{29}$Si magic angle spinning NMR, J. Nucl. Mater. 433 (2013)199-205.

[9] P. Krautwasser, G.M. Begun, P. Angelini, Raman spectral characterization of silicon carbide nuclear fuel coatings, J. Am. Ceram. 66 (1983) 424-434.

[10] International atomic energy agency, fuel performance and fission product behaviour in gas cooled reactors. [online]. (1997) Available at: http://www-pub.iaea.org/MTCD/Publications/PDF/te_978_prn.pdf .

[11] P. Demkowicz, J. Hunn, R. Morris, Preliminary results of post-irradiation examination of the AGR-1 TRISO fuel compacts, in: Proceedings of the HTR 2012, Tokyo, Japan.

[12] P.E. Brown, R.L. Faircloth, Metal fission product behavior in high temperature reactors -$UO_2$ coated particle fuel, J. Nucl. Mater. 59 (1976) 29-41.

[13] H. Nabielek, P.E. Brown, P. Offermann, Silver release from coated particle fuel, Nucl. Technol. 35 (1977)483-493.

[14] R.E. Bullock, Fission-product release during post irradiation annealing of several types of coated fuel particles, J. Nucl. Mater. 125 (1984)304-319.

[15] J.J. van der Merwe, Evaluation of silver transport through SiC during the German HTR fuel program, J. Nucl. Mater. 395 (2009)99-111.

[16] E. Friedland, J.B. Malherbe, N.G. van der Berg, T. Hlatshwayo, A.J. Botha, E. Wendler, W. Wesch, Study of silver diffusion in silicon carbide, J. Nucl. Mater. 389 (2009) 326–331.

[17] T.T. Hlatshwayo , J.B. Malherbe , N.G. van der Berg , L.C. Prinsloo , A.J. Botha, E. Wendler , W. Wesch, Annealing of silver implanted 6H–SiC and the diffusion of the silver, Nucl. Instrum. Methods Phys. Res. B 274 (2012) 120–125.

[18] T.T. Hlatshwayo, J.B. Malherbe , N.G. van der Berg, A.J. Botha, P. Chakraborty, Effect of thermal annealing and neutron irradiation in 6H-SiC implanted with silver at 350° C and 600° C, Nucl. Instrum. Methods Phys. Res. B 273 (2012) 61–64.

[19] H. J. MacLean, R. G. Ballinger, Silver ion implantation and annealing in CVD silicon carbide: the effect of temperature on silver migration, Second Topical

Meeting on High Temperature Reactors 2004 (HTR-2004), Beijing, China, (2004) 22-24.

[20] C. J. McHargue, J. M. Williams, Ion implantation effects in silicon carbide, Nucl. Instrum. Methods Phys. Res. B 80/81 (1993) 889-8894.

[21] A. Heft, E. Wendler, T. Bachmann, E. Glaser, W. Wesch, Defect production and annealing in ion implanted silicon carbide, Mater. Sci. Eng. B 29 (1995) 142-146.

[22] W. Wesch, A. Heft, E. Wendler, T. Bachmann, and E. Glaser, High temperature ion implantation of silicon carbide, Nucl. Instrum. Methods Phys. Res., Sect. B 96 (1995) 335- 338.

[23] M. Ishimaru, S. Harada, T. Motooka, T. Nakata, T. Yoneda, M. Inoue, Amorphization and solid phase epitaxy of high-energy ion implanted 6H-SiC, Nucl. Instrum. Methods Phys. Res., Sect. B 127/128 (1997) 195- 197.

[24] S. Harada, T. Motooka, Recrystallization and electrical properties of MeV P implanted 6H–SiC, J. Appl. Phys. 87 (2000) 2655- 2657.

[25] S.J. Zinkle, V.A. Skuratov, D.T. Hoelzer, On the conflicting roles of ionizing radiation in ceramics, Nucl. Instrum. Methods Phys. Res., B191 (2002) 758- 766.

[26] E.V. Kalinina, V.A. Skuratov, A.A. Sitnikova, E.V. Kolesnikova, A.S. Tregubova, M.P. Scheglov, Structural peculiarities of 4H-SiC irradiated by Bi ions, Semiconductors 41 (2007) 376–380.

[27] T. T. Hlatshwayo, J. H. O'Connell, V. A. Skuratov, E. Wendler, E. G. Njoroge, M. Mlambo, J. B. Malherbe, Comparative study of the effect of swift heavy ion irradiation at 500 $^{o}$C and annealing at 500 $^{o}$C on implanted silicon carbide. RSC Adv, 6 (2016) 68593-68598.

[28] T. T. Hlatshwayo, J. H. O'Connell, V.A. Skuratov, M. Msimanga, R. J. Kuhudzai, E.G. Njoroge, J.B. Malherbe, Effect of Xe ion (167 MeV) irradiation on polycrystalline SiC implanted with Kr and Xe at room temperature, J. Phys. D: Appl. 48 (2015) 465306.

[29] A. Debelle, M. Backman, L. Thome, W. J. Weber, M. Toulemonde, S. Mylonas, A. Boulle, O. H. Pakarinen, N. Juslin, F. Djurabekova, K. Nordlund, F. Garrido,

and D. Chaussende, Combined experimental and computational study of the recrystallization process induced by electronic interactions of swift heavy ions with silicon carbide crystals. Physics Review B 86 (2012)100102.

[30] E. Lo´pez-Honorato, H. Zhang, D. Yang, P. Xiao, Silver diffusion in silicon carbide coatings, J. Am. Ceram. Soc. 94 (2011) 3064–3071.

[31] A. Audren, A. Benyagoub, L. Thome and F. Garrido, Ion implantation of iodine into silicon carbide: influence of temperature on the produced damage and on the diffusion behavior, Nucl. Instrum. Methods Phys. Res. B. 266 (2008) 2810–2813.

[32] B. Leng, H. Ko, T.J. Gerczak, J. Deng, A.J. Giordani, J.L. Hunter Jr, D. Morgan, I. Szlufarska, K. Sridharan, Effect of carbon ion irradiation on Ag diffusion in SiC, J. Nucl. Mater. 471(2016)220-232.

[33] D. D. Osterberg, J. Youngsman, R. Ubic, I. E. Reimanis and D. P. Butt, Recrystallization kinetics of 3C silicon carbide implanted with 400 keV cesium ions, J. Am. Ceram. Soc. 96 (2013) 3290–3295.

[34] Johan B. Malherbe, N. G. van der Berg, A. J. Botha, E. Friedland, T. T. Hlatshwayo, R. J. Kuhudzai, E. Wendler, W. Wesch, P. Chakraborty, E. F. da Silveira, SEM Analysis of Ion Implanted SiC, Nucl. Instrum. Methods Phys. Res. B 315 (2013) 136- 141.

[35] Y. Liu, G. Wang, S. Wang, J. Yang, L. Chen, X. Qin, B. Song, B. Wang and X. Chen, Defect-induced magnetism in neutron irradiated 6H-SiC single crystals, Phys. Rev. Lett. 106 (2011) 087205.

[36] J.F. Ziegler, M.D. Ziegler, J.P. Biersack, SRIM – The stopping and range of ions in matter (2010), Nucl. Instrum. Methods Phys. Res. Sect. B Beam Interact. Mater. Atoms 268 (11–12) (2010) 1818–1823.

[37] W.J. Weber, F. Gao, R. Devanathan, W. Jiang, The efficiency of damage production in silicon carbide, Nucl. Instrum. Methods Phys. Res. B218 (2004) 68.

[38] W.J. Weber, N. Yu, L.M. Wang, Structure and properties of ion-beam-modified (6H) silicon carbide, J. Nucl. Mater. 53 (1998) 253.

[39] L. Z. Liu, J. Wang, X. L. Wu, T. H. Li, and P. K. Chu, Longitudinal optical phonon–plasmon coupling in luminescent 3C–SiC nanocrystal films. Optics Letters 35 (2010) 4024- 4026.

[40] X. Qiang, H. Li, Y. Zhang, S. Tian, J. Wei, Synthesis and Raman scattering of SiC nanowires decorated with SiC polycrystalline nanoparticles. Materials Letters 107 (2013) 315–317.

[41] W. K Burton, N Cabrera and F C. Frank, The growth of crystals and the equilibrium structure of their surfaces. Phil. Trans. Roy. Soc. 243A (1951) 299-358.

[42] J.P. Hirth and G.M. Pound, Coefficients of evaporation and condensation. J. Phys. Chem. 64 (1960) 619–626.

[43] G. Wulff, Xxv. Zur Frage der Geschwindigkeit des Wachsthums und der Auflösung der Krystallflächen, Z. Krist. 34 (1) (1901) 449-530.

[44] N.G. van der Berg, J.B. Malherbe, A.J. Botha and E. Friedland. Thermal etching of SiC, Appl. Surf. Sci, 258 (2012) 5561 -5566.

[45] H.J. MacLean, Silver Transport in CVD Silicon Carbide, PhD Thesis, MIT, Department of Nuclear Engineering, 2004.

[46] X. Geng, F. Yang, N. Rohbeck, and P. Xiao, An original way to investigate silver migration through silicon carbide coating in TRISO particles. J. Am. Ceram. Soc., 97 (2014) 1979–1986.

[47] J.B. Malherbe, P.A. Selyshchev, O.S. Odutemowo, C.C. Theron, E.G. Njoroge, D.F. Langa, T.T. Hlatshwayo, Diffusion of a mono-energetic implanted species with a Gaussian profile, Nucl. Instrum. Methods Phys. Res. B 406 (2017) 708-713.